DNA-Capped Mesoporous Silica Nanoparticles as an Ion-Responsive Release System to Determine the Presence of Mercury in Aqueous Solutions

Yunfei Zhang,[†] Quan Yuan,[†,‡] Tao Chen,[†] Xiaobing Zhang,*[,‡] Yan Chen,[†,‡] and Weihong Tan*[,†,‡]

[†]Center for Research at Bio/Nano Interface, Department of Chemistry and Department of Physiology and Functional Genomics, Shands Cancer Center, UF Genetics Institute and McKnight Brain Institute, University of Florida, Gainesville, Florida 32611, United States

[‡]State Key Laboratory of Chemo/Bio-Sensing and Chemometrics, College of Biology and College of Chemistry and Chemical Engineering, College of Biology, Hunan University, Changsha, 410082, P. R. China

S *Supporting Information*

ABSTRACT: We have developed DNA-functionalized silica nanoparticles for the rapid, sensitive, and selective detection of mercuric ion (Hg^{2+}) in aqueous solution. Two DNA strands were designed to cap the pore of dye-trapped silica nanoparticles. In the presence of ppb level Hg^{2+}, the two DNA strands are dehybridized to uncap the pore, releasing the dye cargo with detectable enhancements of fluorescence signal. This method enables rapid (less than 20 min) and sensitive (limit of detection, LOD, 4 ppb) detection, and it was also able to discriminate Hg^{2+} from twelve other environmentally relevant metal ions. The superior properties of the as-designed DNA-functionalized silica nanoparticles can be attributed to the large loading capacity and highly ordered pore structure of mesoporous silica nanoparticles, as well as the selective binding of thymine-rich DNA with Hg^{2+}. Our design serves as a new prototype for metal-ion sensing systems, and it also has promising potential for detection of various targets in stimulus-release systems.
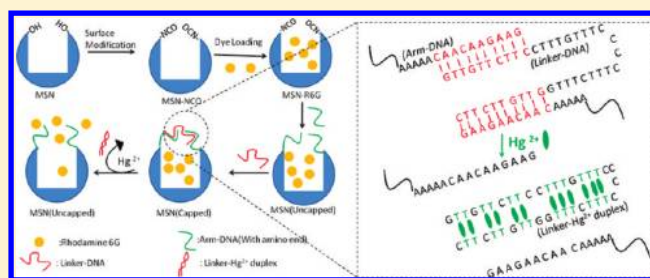
Mercury pollution is a global problem arising from a variety of natural processes and human activities.[1] Because of its high toxicity at low concentration, as well as bioaccumulative effect in the human body, mercury contamination is a continuing concern. Even small amounts of mercury can cause severe damage to the kidney, nervous system, and other organs.[2] Although the accumulation of mercury can be attributed to several sources, the contamination of drinking water by water-soluble Hg(II) is the most common. Therefore, the development of new mercuric ion detection methods that are sensitive, rapid, low-cost, and applicable to aqueous systems has become an urgent need.[3]

Traditional methods for detection of mercuric ion in aqueous systems usually require complicated sample preparation and expensive instrumentation, such as atomic absorption spectroscopy, cold vapor atomic fluorescence spectrometry, and gas chromatography.[3] To simplify sample preparation and reduce instrumentation costs, the development of many mercuric ion detection methods has been based on small organic molecules, such as fluorophores[4] and nanoparticles, such as gold nanospheres,[5−8] or biomaterials, such as DNAzymes,[1] DNA hydrogels,[2] and proteins.[9] Most of the reported approaches rely on direct binding or reaction between the probe and target ion to produce a detectable color or fluorescence change.[10]

This paper reports the direct, rapid, and sensitive detection of mercuric ion (Hg^{2+}) based on a mesoporous silica

nanoparticle -Hg^{2+} responsive dye release system. The unique structure of mesoporous silica nanoparticles (MSN) is used as the dye carrier with a T-base-rich DNA oligomer as an Hg^{2+} responsive cap. Their biocompatibility, large loading capacity, highly ordered pore structure, and adjustable pore size make MSN very suitable as carrier vehicles.[11,12] Furthermore, the silanol group on the surface provides a means of binding an organic or biological linker to a large molecule that is able to cap the pores. Linkers can also be cleaved by a specific stimulus which can uncap the pore and release the cargo.[12] Recent research has demonstrated that MSN can be capped by various materials, including DNA,[13] proteins,[14,15] nanoparticles,[16,17] and polymers,[18−21] and also uncapped by various stimuli, such as heat,[14] magnetic fields,[18] pH,[11,12,17] target molecules,[16,22] enzymes,[19,21,23] or even light.[20] These designs have considerable potential for drug release systems,[12] but there has been very little application of a stimulus-release MSN system for the sensitive detection of target molecules.

Briefly, we designed two DNA strands to cross-link on the surface of dye-trapped MSN in order to cap the pore. In the presence of Hg^{2+}, one DNA strand with higher affinity to Hg^{2+}

is dehybridized from the other strand to uncap the pore. Thus, Hg^{2+} acts as the stimulus to release the dye-trapped MSN, which provides the detection signal in this stimulus-release process. The results show that the new design can achieve rapid and sensitive detection of mercuric ion in aqueous solution, with no significant response to other environmentally important metal ions.

■ EXPERIMENTAL SECTION

Chemicals. The chemicals, including tetraethylorthosilicate (TEOS), *n*-cetyltrimethylammonium bromide (CTABr), 3-(triethoxysilyl)propyl isocyanate (TSPI), sodium hydroxide (NaOH), sodium nitrate (NaNO$_3$), 3-(*N*-morpholino)-propanesulfonic acid (MOPS), Triton X-100, Rhodamine 6G, acetone, mercury(II) acetate(HgAc$_2$), lead(II) acetate (PbAc$_2$), barium acetate (BaAc$_2$), iron(II) acetate (FeAc$_2$), iron(III) chloride (FeCl$_3$), zinc acetate (ZnAc$_2$), magnesium acetate (MgAc$_2$), cadmium acetate (CdAc$_2$), copper(II) acetate (CuAc$_2$), cobalt(II) acetate (CoAc$_2$), nickel(II) acetate (NiAc$_2$), calcium acetate (CaAc$_2$), anhydrous toluene, anhydrous acetonitrile, ethanol, and methanol, were all provided by Sigma-Aldrich. Fluorescein was provided by Invitrogen. Deionized water was obtained from a Milli-Q purification system.

Buffer Solutions. Binding buffer, consisting of 10 mM MOPS, 50 mM NaNO$_3$, and 0.05% (by volume) Triton X-100 (pH = 7.0), was used for DNA binding and dye release tests. Hybridization buffer in 10 mM MOPS, 50 mM NaNO$_3$, and 20 mM MgAc$_2$ (pH = 7.0) was used for DNA hybridization.

Preparation of Mesoporous Silica Nanoparticles (MSN). Mesoporous silica particles were synthesized according to the published protocol.[24] A 500 mg sample of *n*-cetyltrimethylammonium bromide (CTABr) was dissolved and suspended in 250 mL of DI water, followed by addition of 3.5 mL of NaOH (1M). The CTABr solution was transferred to a 500 mL, 3-necked flask and heated to 80 °C with magnetic stirring. Next, 2.5 mL of tetraethylorthosilicate (TEOS) was added dropwise to the CTABr solution. The solution was allowed to react for 2 h with magnetic stirring to obtain a white powder precipitate. The mixture was cooled to room temperature and then centrifuged at 2000 rpm for 10 min to eliminate the supernatant. The solid was washed with ethanol three times. The final product was refluxed in methanol for 20 h to eliminate CTABr. After washing with ethanol three times, the mesoporous silica nanoparticle (MSN) product was obtained and kept dry under ambient conditions.

Synthesis of Isocyanate-Functionalized Mesoporous Silica Nanoparticles (MSN-NCO) and Dye Loading. A 500 mg sample of the extracted MSN was refluxed in 80 mL of anhydrous toluene with 0.25 mL of 3-(triethoxysilyl)propyl isocyanate(TSPI) for 20 h to immobilize the isocyanate group on the surface. The isocyanate-functionalized MSN (MSN-NCO) was collected and washed with anhydrous toluene three times and then dried in an oven at 70 °C to evaporate the toluene. Next, 500 mg of functionalized MSN-NCO was suspended in 20 mL of Rhodamine 6G/acetone saturated solution inside a 50 mL centrifuge tube to load the dye into the pores of the MSN-NCO scaffolding. The mixture was ultrasonicated for 1 min and then shaken for 24 h to achieve maximum dye loading. Afterward, the dye-loaded MSN-NCO was washed quickly with acetone three times and dried in an oven at 70 °C. The dye-loaded MSN (MSN-R6G) was kept dry until the next step.

Materials Characterization. Characterization of the size and morphology of the MSN was performed using an Hitachi-7000 transmission electron microscope (Tokyo, Japan). High resolution electron microscopy digital images were recorded with a CCD camera. Samples were prepared by placing one drop of an initial water solution of nanoparticles onto a copper grid. The sample was dried overnight at room temperature before TEM investigation; photos were then taken. SEM characterization of MSN was performed using scanning electron microscopy (SEM) (JEOL JSM-6700). High resolution electron microscopy digital images were recorded with a CCD camera. The elemental compositions of the MSN and MSN-NCO were determined by elemental analysis. The nitrogen adsorption and desorption isotherms of MSN and MSN-R6G were measured at 78.3 K using an ASAP 2010 analyzer (Micromeritics). The BET model was applied to evaluate the specific surface areas. Pore size and pore volume were determined from the adsorption data by the BJH method. XRD patterns of MSN, MSN-NCO, and dye-doped MSN were recorded on a D/MAX-2000 diffractometer (Rigaku), using Cu Kα radiation (λ = 1.5406 Å).

Synthesis and Purification of Arm-DNA and Linker-DNA. The designed DNA sequences were synthesized using a DNA/RNA synthesizer (ABI3400, Applied Biosystems). The sequences were

> Arm-DNA: 5'-GAA GAA CAA CAA AAA-NH$_2$-3'
>
> Linker-DNA: 5'-GTT GTT CTT CCT TTG TTT CCC CTT TCT TTG GTT GTT CTT C-3'
>
> Fluorophore-Linker-DNA: 5'-FAM-GTT GTT CTT CCT TTG TTT CCC CTT TCT TTG GTT GTT CTT C-Dabcyl-3'
>
> Complementary-Linker-DNA: 5'-G AAG AAC AAC CAA AGA AAG GGG AAA CAA AGG AAG AAC AAC-3'

The synthesized DNA was purified by HPLC and then dissolved in water. The DNA concentration was determined by absorbance measurements on a Cary Bio-300 UV spectrometer (Varian). The DNA solution was dried, and the DNA was kept in a −20 °C freezer until use.

Attachment of Amino-Modified Arm-DNA on Dye-Loaded Isocyanate-Functionalized Mesoporous Silica Nanoparticles (MSN-R6G). Synthesized amino-modified Arm-DNA was resuspended in anhydrous acetonitrile. A series of volumes (2, 4, 8, 12, 16, 20, and 24 μL) of 1 mM amino-modified Arm-DNA solution was added to 1 mg of MSN-R6G in 1.5 mL centrifuge tubes, followed by adjustment of the total volume to 30 μL with anhydrous acetonitrile. An individual pipet tip was used for each tube for rapid mixing. The solution was agitated at room temperature for 30 min; then, binding buffer was added to adjust the overall volume to 200 μL. The mixture was shaken for 1 more hour at room temperature (1000 rpm). After centrifugation, the absorbance of each supernatant was measured to calculate the amount of Arm-DNA attached on the MSN. The MSN-Arm-DNA conjugate was obtained and washed twice with binding buffer. From Figure S-1 (Supporting Information), 12 nmol of Arm-DNA was determined to be the optimal amount to saturate the surface of 1 mg of MSN-R6G, giving a final yield of 10 nmol of Arm-DNA per mg of MSN-R6G.

In order to obtain solid MSN-Arm-DNA, 6 μL of 1 mM Arm-DNA solution was quickly added to 500 μg of dry MSN-R6G powder. Anhydrous acetonitrile (24 μL) was added, and a pipet tip was used to mix. After shaking this mixture for 30 min, binding buffer was added to adjust the final volume to 200 μL.

Scheme 1. (A) Schematic Representation of the Synthesis, Surface Modification, Dye Loading, and DNA Binding of the MSN, as well as the Release of Dye from MSN in the Presence of Mercuric Ion. (B) Hybridization of the Arm-DNA and Linker-DNA in the Absence and Presence of Mercuric Ion[a]
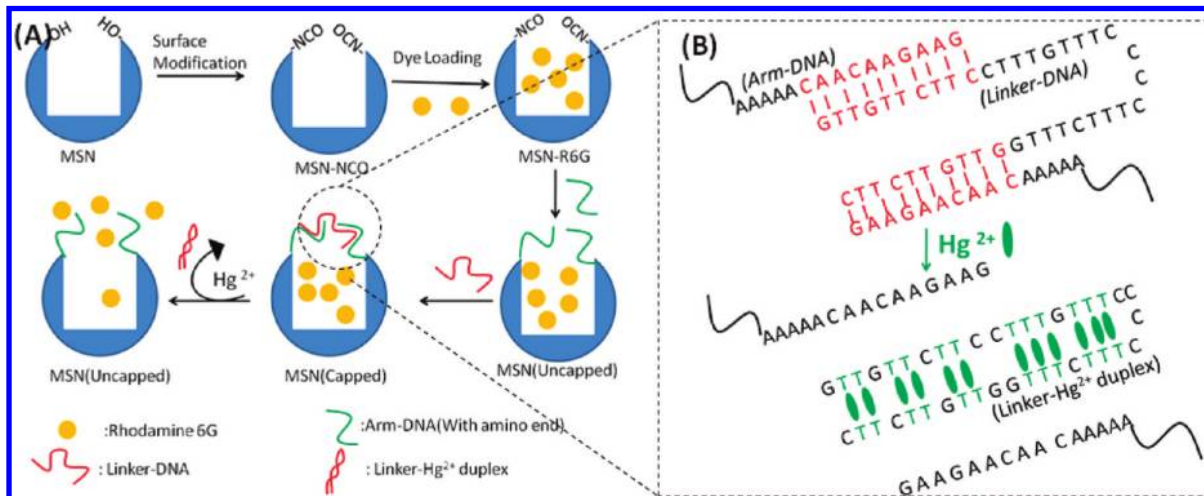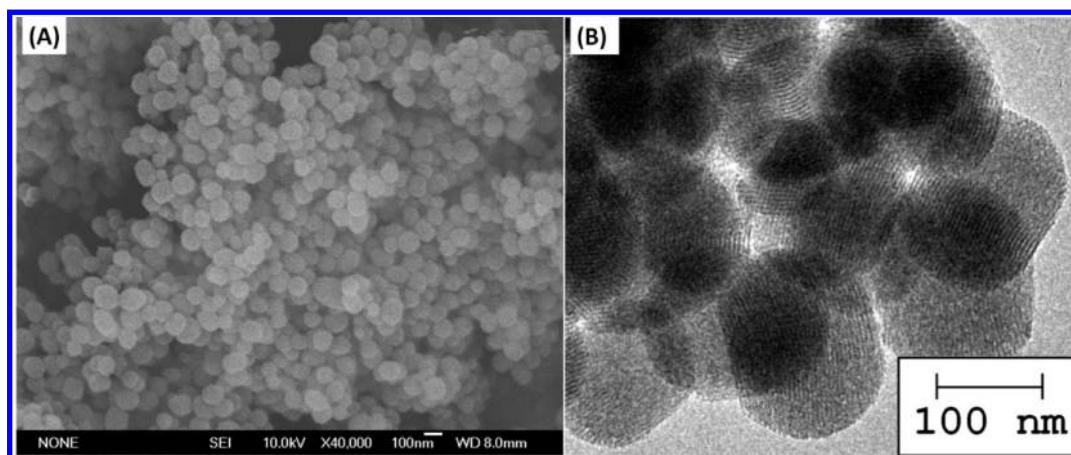

[a]Green dot: mercuric ion.

Figure 1. (A) SEM image of solid MSN, showing the spherical morphology. (B)TEM image of solid MSN, showing the highly ordered porous structure.

The suspension was shaken for 1 h (1000 rpm, room temperature). The solution was quickly centrifuged and washed with binding buffer three times to minimize the free release of the Rhodamine 6G. The absorbance of the supernatant was measured to calculate the binding efficiency of Arm-DNA, which was in the range of 86 to 91%.

Hybridization of Arm-DNA and Linker-DNA. The MSN-Arm-DNA solid was prepared as described above. The Linker-DNA was introduced to hybridize with the Arm-DNA immobilized on the MSN. MSN-Arm-DNA solid (500 μg) was suspended in 200 μL of hybridization buffer containing 20 nmol of Linker-DNA. The solution was shaken on an Eppendorf Thermomixer for 2 h (1000 rpm, room temperature) and then centrifuged and washed with binding buffer three times. The absorbance of the supernatant was measured to calculate the hybridization efficiency of Linker-DNA to Arm-DNA. On the basis of the results, 22.4%−23.3% of the Linker-DNA was hybridized to the Arm-DNA, giving a ratio of Linker-DNA to Arm-DNA on the MSN from 2.23:1.00 to 2.14:1.00, as one Linker-DNA strand will bridge-link two Arm-DNA strands on the surface of the MSN.

Dye Release Experiment. After the hybridization step of Arm-DNA and Linker-DNA, the excess Linker-DNA was removed by washing and centrifugation. In order to monitor the dye release curve of this system in the presence of mercuric ions, 0.5 mg of Linker-DNA-capped MSN-R6G was suspended in mercuric acetate/binding buffer solution of different concentrations (0, 2, 10, 20, 50, 100, 200, and 500 ppb and 1 ppm). To avoid having to remove suspended particles before fluorescence measurements, the particles were suspended in 200 μL of mercuric solution of the appropriate concentration in a Mini Dialysis Filter (Thermo Scientific, MW cutoff of 7000) with a small piece of foam floating on the surface of 5 mL of mercuric solution in a 10 mL beaker (Figure S-3, Supporting Information). The solution was continuously stirred with a magnetic stir bar at 400 rpm at room temperature, and 150 μL volumes of solution were taken from the beaker to measure the fluorescence intensity (HORIBA, Jobin Yvon) every 5 min.

In order to test the maximum dye release of this system, 0.5 mg of Linker-DNA-capped MSN-R6G was incubated with an excess amount of the Linker-DNA, and the dye release curve
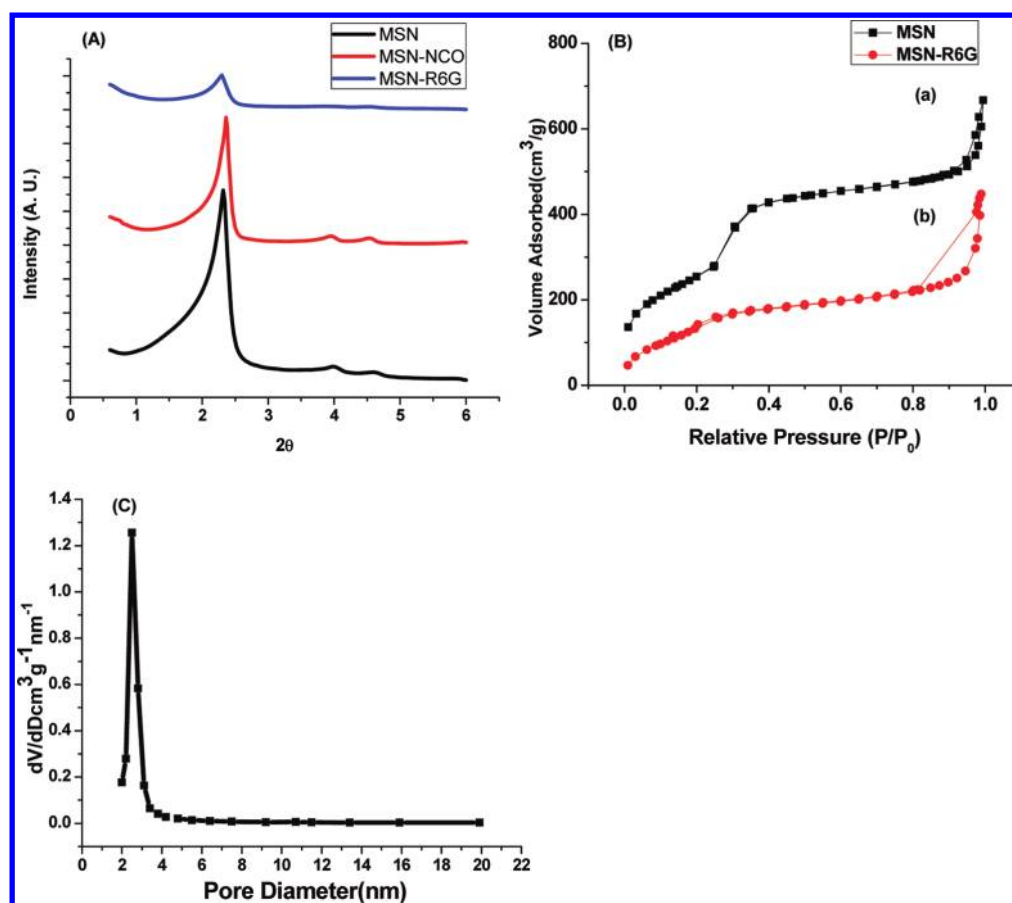
Figure 2. (A) Powder X-ray patterns of the solids: MSN as synthesized and calcined, isocyanate group-functionalized MSN, and Rhodamine 6G-doped MSN-NCO. (B) BET nitrogen adsorption/desorption isotherms of the solids (a) MSN as synthesized and calcined and (b) MSN after dye doping with Rhodamine 6G. (C) BJH pore size distribution of MSN.

was also monitored. The dye release curve is shown in Figure S-4, Supporting Information.

RESULTS AND DISCUSSION

Detection Mechanism. The stimulus-release process is illustrated in Scheme 1A. The solid MSN were first functionalized with isocyanate groups (denoted as MSN-NCO). The functionalized MSN-NCO were then loaded with Rhodamine 6G, which has shown relatively low quenching compared to other organic dyes (see Figure S-2, Supporting Information), to obtain the dye-trapped MSN (denoted as MSN-R6G). A short DNA strand with amino group at the 3′ end (5′-GAA GAA CAA CAA AAA-NH$_2$-3′, denoted as Arm-DNA) was then added to the MSN-R6G suspension to bind the surface by reaction of the isocyanate (−NCO) and amino(−NH$_2$) groups. Because the flexibility of the single-stranded DNA (cross-sectional diameter = 0.6 nm) displayed poor coverage of the MSN pores,[25] the MSN particles remained "uncapped" at this stage. Thus, in the next step, after removing excess Arm-DNA, T-base-rich Linker-DNA (5′-GTT GTT CTT CCT TTG TTT CCC CTT TCT TTG GTT GTT CTT C-3′) was introduced to hybridize with the Arm-DNA. Linker-DNA has two binding sites with the Arm-DNA, causing it to cross-link the Arm-DNA on the MSN surface. The cross-links result in significant closure of the pores and inhibition of dye release in the absence of target Hg^{2+}.

Scheme 1B shows that Arm-DNA partially hybridizes with Linker-DNA, leaving 12 T bases unhybridized. Previous

research has shown that mercuric ion can bind to two thymine bases to form the stable T-Hg^{2+}-T duplex.[1] Thus, in the presence of mercuric ion, the Linker-DNA prefers to form the more stable T-Hg^{2+}-T intramolecular duplex structure and therefore dehybridizes from the Arm-DNA. This action, whereby the Linker-DNA Hg^{2+} duplex leaves the MSN, effectively uncaps the MSN pore to release the dye, and a fluorescence signal is produced.

Characterization of Synthesized and Dye-Doped MSN. The morphology of the mesoporous silica nanoparticles was characterized by SEM and TEM. The SEM image (Figure 1A) shows a homogeneous spherical structure with diameter around 100 nm. The TEM image (Figure 1B) shows the homogeneous porosity of MSN with pore size of about 2.5 nm. The elemental composition of the MSN before and after surface modification was measured by elemental analysis (data shown in Supporting Information Table S-1) to indicate the surface modification of mesoporous silica nanoparticle. The homogeneous porosity of MSN, MSN-NCO, and MSN-R6G was also confirmed by X-ray diffraction (Figure 2A). The X-ray patterns of these mesoporous solid particles did not show any peak shift during the surface modification and dye loading processes, indicating that the porous property of MSN remained unchanged. The nitrogen adsorption−desorption isotherms of MSN and MSN-R6G also show typical curves for these mesoporous solids (Figure 2B). The surface adsorption of nitrogen was significantly reduced after the dye doping process. On the basis of the analyzed data, the BET surface area was
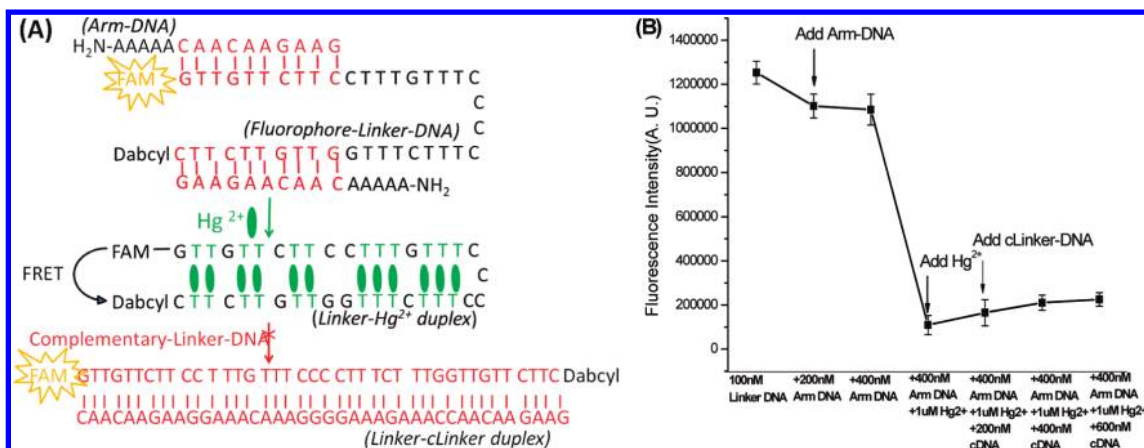
Figure 3. (A) Hybridization between Arm-DNA, Fluorophore-Linker-DNA, and Complementary-Linker-DNA in the presence of Hg^{2+}.(B) Fluorescence intensity of the 100 nM Fluorophore-Linker-DNA solution after the addition of the indicated concentrations of Arm-DNA, Hg^{2+} and Complementary-Linker-DNA.
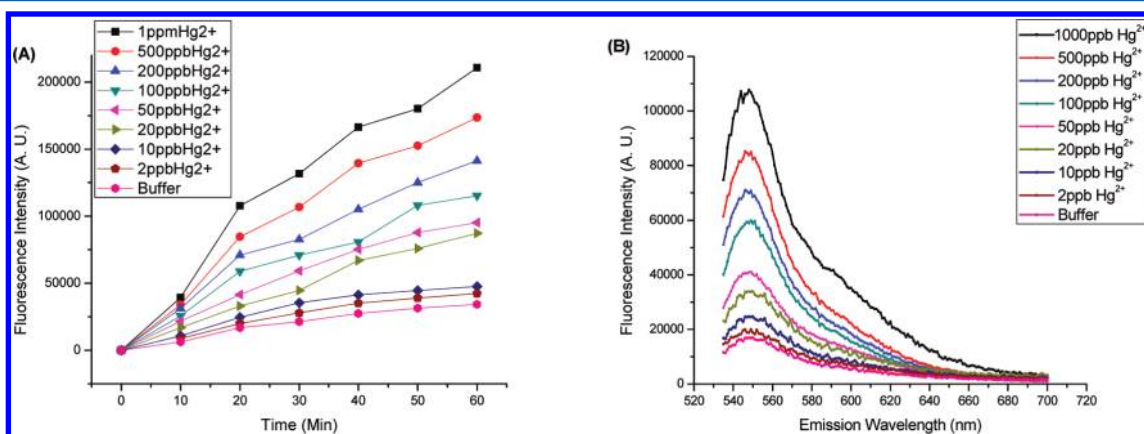

Figure 4. (A) Release curve of Rhodamine 6G from Linker-DNA-capped MSN-R6G with different concentrations of Hg^{2+}. (B) Fluorescence signal 20 min following dye release in the presence of Hg^{2+}. Laser excitation wavelength: 520 nm.

reduced from 934 to 537 m^3/g during dye doping. Moreover, pore volume was reduced from 1.032 to 0.692 cm^3/g, indicating the successful trapping of Rhodamine 6G in the particles. Also, the BJH pore size distribution of the MSN was analyzed, and the average pore diameter of MSN was 2.5 nm.

Evidence for the Formation of Linker-DNA Hg^{2+} Duplex. To verify that the mercuric ion can efficiently break the hybridization between Arm-DNA and Linker-DNA, hybridization tests using free DNA strands in solution were performed. A fluorophore and a quencher were added on opposite ends of Linker-DNA (5′-FAM-GTT GTT CTT CCT TTG TTT CCC CTT TCT TTG GTT GTT CTT C Dabcyl-3′, denoted as Fluorophore-Linker-DNA). As shown in Figure 3A, by itself or in the presence of Arm-DNA, there was no fluorescence resonance energy transfer (FRET), and the fluorescence intensity was high. However, upon addition of Hg^{2+} and formation of the intramolecular duplex, FRET occurred, and the fluorescence was quenched. In the fluorescence test, an excess amount of Arm-DNA was added to the Fluorophore-Linker-DNA. In the 2002 report by Nazarenko,[26] a duplex formed by a single G-C base pair resulted in significant quenching of fluorescence on the nearby fluorescein. In Figure 3B, a small decrease in fluorescence was detected after the addition of Arm-DNA, corresponding to G-C pair formation next to the fluorescein, indicating duplex formation between the Arm-DNA and fluorophore-Linker-

DNA. Afterward, this solution was titrated with mercuric ion. A significant fluorescence reduction was observed, indicating that mercuric ions could efficiently destroy the Linker-Arm intermolecular hybridization and form the new Linker-Hg^{2+} intramolecular duplex. Subsequently, excess cDNA complementary to the Linker-DNA (cLinker-DNA: 5′-GAA GAA CAA CCA AAG AAA GGG GAA ACA AAG GAA GAA CAA C-3′) was introduced. The Linker-cLinker complex is very stable with a melting point as high as 63.9 °C (calculated by the Integrated DNA Technologies Web site). However, in this test, even this cDNA could hardly open the Linker-DNA Hg^{2+} duplex, and only a small increase of fluorescence intensity was detected. This result showed that Hg^{2+} could easily destroy the hybridization between Arm-DNA and Linker-DNA and form a very stable Linker-DNA-Hg^{2+} structure at room temperature, indicating that Hg^{2+} is a good stimulus to uncap the MSN pore and release the trapped dye molecules.

Detection of Hg^{2+} Ion in Aqueous Solution. The key advantage of this stimulus-release system is the signal amplification process. Because of the unique hollow structure and large inner space of MSN, a large number of dye molecules can be trapped, but only a small concentration of the "key" molecule (Hg^{2+} in this paper) is required to uncap an MSN pore and release a large amount of dye molecules to generate a high fluorescence signal. In the test, a 0.5 mg sample of Linker-DNA capped MSN-R6G was dispersed in mercuric acetate

1960

dx.doi.org/10.1021/ac202993p | Anal. Chem. 2012, 84, 1956–1962

solution of different concentrations (0, 2, 10, 20, 50, 100, 200, and 500 ppb and 1 ppm). To avoid having to remove suspended particles before fluorescence measurements, the particle slurry was suspended in a Mini Dialysis Filter (MW cutoff at 7000) with a small piece of foam floating on the surface of 5 mL of mercuric solution of the same concentration (Figure S-3, Supporting Information). Aliquots were taken from the beaker to observe the dye release according to the fluorescence intensity change, as graphed in Figure S-4, Supporting Information.

In accordance with the sensor's working principle, the capped MSN were uncapped in the presence of Hg^{2+}, and the release of Rhodamine 6G, which increased with increasing concentrations of Hg^{2+}, was detected. The kinetic curve of the dye release with different concentrations of Hg^{2+} is shown in Figure 4A. In order to minimize nonspecific leaking of the dye molecule from the particles, 20 min was chosen as the detection time point. Figure 4B shows the fluorescence signal 20 min following dye release for a series of Hg^{2+} concentrations. The signals for samples from 0 to 100 ppb gave a linear fit (Figure
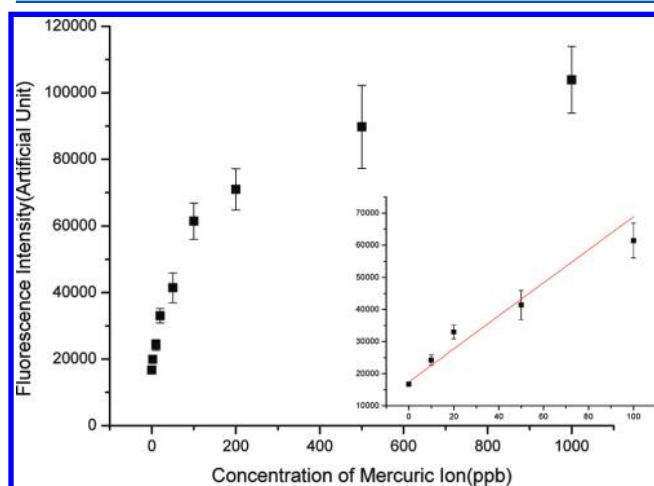

Figure 5. Fluorescence emission signal in the presence of increasing amounts of mercuric ion. Inset: Linear fit of the fluorescence signal, slope = $(1.76 \pm 0.06) \times 10^4$ ppb^{-1}; intercept = (512 ± 44). Excitation at 520 nm; emission at 550 nm.

5), and the calculated detection limit was 4 ppb Hg^{2+}. The low limit of detection (LOD) and rapid response indicate that this method can be a high-throughput and sensitive process for the detection of Hg^{2+}.

The calibration curve of the fluorescence intensity of Rhodamine 6G dye was measured and used to calculate the amount of the released dye (Figure S-4, Supporting Information). From the calculation results, 2 ppb of mercuric ion leads to 9.5-fold amplification of the amount of dye released from the nanoparticle (calculation process in Supporting Information Table S-2). Additional studies using cDNA to the Linker-DNA (cLinker-DNA 5′-GAA GAA CAA CCA AAG AAA GGG GAA ACA AAG GAA GAA CAA C-3′) were performed to test the maximum opening of these systems. As shown in Figure S-5 (Supporting Information), MSN-R6G was tightly capped by Linker-DNA with only negligible release of Rhodamine 6G in the absence of mercuric ion, while in the presence of cLinker-DNA, a large release of dye molecule was observed.

To assess potential interference by other metal ions, the Linker-DNA-capped MSN-R6G particles were also tested in 1 ppm solutions of lead(II) acetate (PbAc$_2$), barium acetate (BaAc$_2$), iron(II) acetate (FeAc$_2$), iron(III) chloride (FeCl$_3$), zinc acetate (ZnAc$_2$), magnesium acetate (MgAc$_2$), cadmium acetate (CdAc$_2$), copper(II) acetate (CuAc$_2$), cobalt(II) acetate (CoAc$_2$), nickel(II) acetate (NiAc$_2$), and calcium acetate (CaAc$_2$). The dye release was observed using the same process as described before, and the fluorescence intensity 20 min after release was measured compared to the buffer control. As shown in Figure 6, in this specific stimulus-response dye release
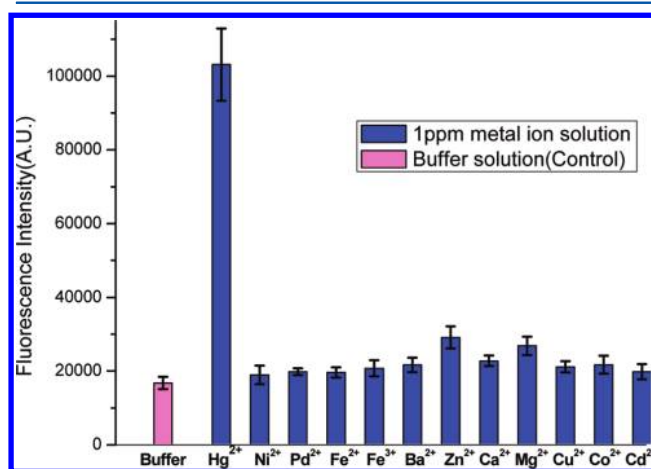

Figure 6. Fluorescence intensities of the released dye from Linker-DNA-capped MSN-R6G in the presence of 1 ppm of different cations. Release time: 20 min.

system, no interference from other metal ions occurred, with the 1 ppm Hg^{2+} solution producing an average of 6.2 times the fluorescence intensity of the buffer control.

■ CONCLUSIONS

In conclusion, we have designed a new MSN-based Hg^{2+} responsive dye release system to achieve direct, rapid, sensitive detection of Hg^{2+} in aqueous solution. The specific binding affinity between Hg^{2+} and T-rich DNA enabled the design of a DNA-capped MSN which is responsive only to Hg^{2+}. Opening the pore leads to the release of a large amount of dye cargo, resulting in large signal amplification. Results showed that this design can achieve rapid (less than 20 min) and sensitive (LOD 4 ppb) detection of mercuric ion in aqueous solution. Selectivity tests showed no potential interference by other metal ions. Although there are some device-dependent ion detection techniques with better detection limits,[27] this method has low instrumentation cost and easy operation. Since this DNA-capped MSN can be easily maintained and detection can be simply operated, we strongly believe that this approach shows promise as a prototype for the development of a new metal-ion sensing system. Although our design may not have the significant advantage in LOD compared to some other reported approaches due to the nonspecific leaking of the dye molecule in buffer, this is an encouraging starting point for use of the mesoporous-DNA stimulus-release system as a target molecule detection method.[8] With the specific interaction between certain DNA strands (e.g., aptamers[28]) and their target molecules, this design may also be applicable for the detection of variety of targets via the stimulus-release process.

■ ASSOCIATED CONTENT

S Supporting Information

Additional information as noted in text. This material is available free of charge via the Internet at http://pubs.acs.org.

■ AUTHOR INFORMATION

Corresponding Author

*Fax: +1 352 846 2410. E-mail: tan@chem.ufl.edu (W.T.); xiaobingzhang89@hotmail.com (X.Z.).

■ ACKNOWLEDGMENTS

■ REFERENCES

(1) Li, T.; Dong, S.; Wang, E. *Anal. Chem.* **2009**, *81*, 2144−2149.

(2) Dave, N.; Chan, M. Y.; Huang, P.-J.J.; Smith, B. D.; Liu, J. *J. Am. Chem. Soc.* **2010**, *132*, 12668−12673.

(3) Nolan, E.; Lippard, S. *Chem. Rev.* **2008**, *108*, 3433−3480.

(4) Chiang, C.; Huang, C.; Liu, C.; Chang, H. *Anal. Chem.* **2008**, *80*, 3716−3721.

(5) Lee, J.; Mirkin, C. A. *Anal. Chem.* **2008**, *80*, 6805−6808.

(6) Lee, J.; Han, M. S.; Mirkin, C. A. *Angew. Chem., Int. Ed.* **2007**, *46*, 4093−4096.

(7) Xue, X. J.; Wang, F.; Liu, X. G. *J. Am. Chem. Soc.* **2008**, *130*, 3244−3245.

(8) Li, M.; Wang, Q. Y.; Shi, X. D.; Hornak, L. A.; Wu, N. Q. *Anal. Chem.* **2011**, *83*, 7061−7065.

(9) Chen, P.; He, C. *J. Am. Chem. Soc.* **2004**, *126*, 728−729.

(10) Climent, E.; et al. *Angew. Chem., Int. Ed.* **2009**, *48*, 8519−8522.

(11) Chen, C.; et al. *Nucleic Acids Res.* **2011**, *39*, 1638−1644.

(12) Lee, C.; et al. *Angew. Chem., Int. Ed.* **2010**, *49*, 8214−8219.

(13) Climent, E.; et al. *Angew. Chem., Int. Ed.* **2010**, *49*, 7281−7283.

(14) Schlossbauer, A.; et al. *Angew. Chem., Int. Ed.* **2010**, *49*, 4734−4737.

(15) Schlossbauer, A.; Kecht, J.; Bein, T. *Angew. Chem.* **2009**, *121*, 3138−3141.

(16) Zhu, C.; Lu, C.; Song, X.; Yang, H.; Wang, X. *J. Am. Chem. Soc.* **2011**, *133*, 1278−1281.

(17) Liu, R.; et al. *J. Am. Chem. Soc.* **2010**, *132*, 1500−1501.

(18) Thomas, C. R.; et al. *J. Am. Chem. Soc.* **2010**, *132*, 10623−10625.

(19) Patel, K.; et al. *J. Am. Chem. Soc.* **2008**, *130*, 2382−2383.

(20) Park, C.; Lee, K.; Kim, C. *Angew. Chem., Int. Ed.* **2009**, *48*, 1275−1278.

(21) Park, C.; Kim, H.; Kim, S.; Kim, C. *J. Am. Chem. Soc.* **2009**, *131*, 16614−16615.

(22) Zhao, Y.; Trewyn, B. G.; Slowing, I. I.; Lin, S. Y. *J. Am. Chem. Soc.* **2009**, *131*, 8398−8400.

(23) Bernardos, A.; et al. *Angew. Chem.* **2009**, *121*, 5598−6001.

(24) Beck, J. S.; et al. *J. Am. Chem. Soc.* **1992**, *114*, 10834−10843.

(25) Cuie Chen.; et al. *Nucleic Acids Res.* **2011**, *39*, 1638−1644.

(26) Nazarenko, I.; Pires, R.; Lowe, B.; Obaidy, M.; Rashtchian, A. *Nucleic Acids Res.* **2002**, *30*, 2089−2095.

(27) Chen, J.; Chen, H.; Jin, X.; Chen, H. *Talanta* **2009**, *77*, 1381−1387.

(28) Zhang, Y.; Chen, Y.; Han, D.; Ocsoy, I.; Tan, W. *Bioanalysis* **2010**, *2*, 907−918.